

Photocatalytic Degradation of Methylene Blue Dye Using Zinc Oxide Nanoparticles Prepared by Green Synthesized

Anwar Ali Baqer^{1*}  , Nadia Jasim Ghdeeb²  , Nedal Ali Hussain²  

¹Department of Physics, College of Science for Women, University of Baghdad, Baghdad, Iraq

²Department of Physics, College of Science, University of Mustansyriah, Baghdad, Iraq

*Corresponding Author.

Received 18/01/2024, Revised 04/05/2024, Accepted 06/05/2024, Published Online First 20/12/2024



© 2022 The Author(s). Published by College of Science for Women, University of Baghdad.

This is an open-access article distributed under the terms of the [Creative Commons Attribution 4.0 International License](https://creativecommons.org/licenses/by/4.0/), which permits unrestricted use, distribution, and reproduction in any medium, provided the original work is properly cited.

Abstract

This study describes the environmentally friendly synthesis of zinc oxide nanoparticles (ZnO-NPs) using cinnamon extract, bay leaf extract, and chemical techniques. Due to its cost-effectiveness and avoidance of harmful ingredients, the green synthesis strategy for producing nanoparticles has significant advantages over physical and chemical procedures. The XRD data demonstrated the production of a hexagonal wurtzite structure, while the SEM investigations demonstrated a spherical shape and average size (21.49, 25.26) nm for ZnO NPs synthesized by cinnamon extract, bay leaf extract, and chemical techniques, respectively. The synthesized ZnO NPs demonstrate noteworthy photocatalytic efficacy in the breakdown of methylene blue dye under direct sunlight exposure. Therefore, this research signifies a significant advancement in the progress of a sustainable photocatalyst to eliminate harmful dyes from water.

Keywords: Chemical synthesis, Green synthesis, Nanoparticles, Photocatalytic degradation, ZnO.

Introduction

Currently, industrial development has generated a large number of pollutants which are released into the environment. On the other hand, a large number of pollutants in the form of heavy metals, organic pigments, and microorganisms are released daily into water systems for example, chromophores found in dye molecules, indigo, azo, phenol, and triphenylmethane compounds are harmful to aquatic environments and humans¹. It has been proposed to remove organic pollutants from water, including coagulation coupled with sedimentation, biological processes, membrane filtration, adsorption, advanced oxidation, catalysis, and photocatalysis²⁻⁴. In this regard, various techniques are used to employ semiconducting nanomaterials to remove these organic pollutants, such as electroplating and

photocatalysis. However, photocatalysis is widely adopted due to its easy approach, cost-effectiveness, no side product, and use of untapped solar spectrum⁵. These advantages include enhanced utilization of solar radiation, cost-effectiveness, and the potential for facile recovery of the photocatalyst in powder form through specific processes, or without any additional steps in the case of thin films. Numerous electronic components have been employed for this particular objective; but, the photocatalyst that has received the most extensive research attention is TiO₂, primarily owing to its exceptional physicochemical characteristics. Notably, TiO₂ has demonstrated the highest level of efficiency in the anatase phase. Nevertheless, zinc oxide (ZnO) has emerged as a widely utilized photocatalyst for water

purification, among other photocatalysts^{2,3}. The semiconductor under consideration possesses a significant band gap of 3.3 electron volts (eV). Solar cells, gas sensors^{4,5}, and dye degradation are among the various applications of this technology⁶. Zinc oxide nanoparticles have been synthesized by a range of chemical and physical methodologies, such as Sol-Gel⁷, precipitation⁸, arc discharge⁹, hydrothermal¹⁰, and pulsed laser ablation¹¹. For the synthesis of zinc oxide nanoparticles, a green synthesis method has been utilized due to its many advantages over physical and chemical methods, as it does not entail hazardous chemicals, is environmentally friendly, and is cost-effective^{12,13}. It utilizes biological materials that are readily extracted from vegetation.¹⁴

These phytoconstituents function as stabilizing and reducing agents and catalyze the chemical reduction of nanoparticles of metal oxide. According to our knowledge, no report exists on the use of cinnamon extract, or bay leaf extract in the synthesis of ZnO nanoparticles (NPs) as shown in Fig 1. The food, paper, leather, and textile industries utilize organic compounds known as dyes. The discharges from these industrial operations consist of dyes that are

both highly pigmented and poisonous. The discharge of effluents presents a significant risk to the well-being of aquatic organisms, humans, animals, and the surrounding ecosystem due to the contamination of both surface and groundwater sources. Before release, it is imperative to subject the effluent to treatment to facilitate the degradation of the dye into a non-toxic form. A range of purifying approaches, including physical, chemical, and biological methods, have been developed to address different types of pollutants. The utilization of ZnO NPs proved to be successful in the degradation of dyes¹⁵⁻¹⁷. Methylene Blue (MB) is an intensely colored compound which is used in dyeing and printing textiles and is a common water pollutant.

The present investigation involved the production of ZnO NPs through the utilization of a green synthesis approach. Green methods are easy, cheap and environmentally safe methods that are manufactured using plant extracts. Employing leaf extract derived from cinnamon, bay leaf. The utilization of green ZnO NPs has been seen in the process of photocatalytic degradation of methylene blue MB blue dye under direct sunlight exposure.

Materials and Methods

Materials

Cinnamon, bay leaf, zinc acetate dihydrate [$\text{Zn}(\text{CH}_3\text{COO})_2 \cdot 2\text{H}_2\text{O}$]

Preparation Methods

As a solvent, cinnamon, bay leaf, zinc acetate dihydrate [$\text{Zn}(\text{CH}_3\text{COO})_2 \cdot 2\text{H}_2\text{O}$], and 99% purity are used. First, cinnamon is minced. Use distilled water to rinse. After that, bay leaf, and then left to dry, weigh 20 grams of cinnamon and bay leaf and combine them with deionized water. After 15 minutes of boiling, various aqueous extracts were obtained and deposited in separate beakers. The groups were then filtered through filter paper and stored at 40 °C.

In a beaker, zinc acetate (0.1 M) was dissolved in 50 mL of deionized water, which was magnetically stirred for 15 minutes until

homogeneous. Cinnamon preparations (10 ml) were mixed with it, as were bay leaf preparations (10 ml), each of which was mixed with it. Before the test, 10 mL of a $\text{Zn}(\text{CH}_3\text{COO})_2 \cdot 2\text{H}_2\text{O}$ solution was magnetically stirred for 10 minutes in a beaker and allowed to stand for 24 hours at the chamber temperature.

Before use, the synthesized nanoparticles were spun for 10 minutes at 6000 rpm and washed with ethanol and distilled water. After collecting samples, they were transferred to a Petri dish and desiccated in a vacuum oven at 100 degrees Celsius for four hours.

Nanoparticles (ZnO) were prepared in a simple chemical method using zinc acetate whose chemical symbol ($\text{Zn}(\text{CH}_3\text{COO})_2 \cdot 2\text{H}_2\text{O}$) was furnished by a German company. Its solution was prepared by dissolving (0.1M) of ($\text{Zn}(\text{CH}_3\text{COO})_2$) salts in 50 ml of deionized water.



Figure 1. Process steps for preparing ZnO NPs by chemical and green methods.

Photocatalytic behavior of ZnO NPs

Due to their high photocatalytic activity^{8, 18}, ZnO nanoparticles can be used as photocatalysts. The Photodegradation experiment was carried out and done under natural sunlight in June between 11:30 am and 2 pm. The intensity of solar radiation was 13.654MJ and the time interval during removing the sample from the beaker was one hour in this study, 50 mg L1 solution in water of MB dye with a

5 mg/20 mL ZnO NP catalytic dose in this study. UV absorbance was measured at 0 minutes, 15 minutes, 30 minutes, 45 minutes, 60 minutes, and 75minutes after combining the two solutions (dye and catalyst). Absorbance was plotted using a UV-vis spectrophotometer. Following every time interval, the absorbance decreased, suggesting that ZnO NPs degraded the dye.

Results and Discussion

XRD analysis

Fig 2 depicts the XRD patterns of ZnO NPs produced by chemical synthesis, cinnamon, and bay leaf. The peaks observed in the orientation planes at (100), (002), (101), (102), (110), (103), and (112) correspond to 2θ values of 31.7°, 34.3°, 36.2°, 47.3°, 56°, 62.4°, and 67.8°, respectively for all samples. The statement aligns with the findings of the researchers¹⁹. Higher intensity of diffraction peaks by using bay leaf as shown below. The XRD results revealed that ZnO nanoparticles had a hexagonal wurtzite structure and were highly crystalline. The hexagonal wurtzite structure is analogous to JCPDC Standard Card No. 1314.13.2, proving that ZnO-NPs were effectively synthesized using a green synthesis technique. The ZnO crystal size presented in Table 1

(14–22 nm) was obtained from the XRD spectrum using the Debye–Scherer Equation²⁰:-

$$D = \frac{0.9\lambda}{\beta \cos \theta} \dots\dots\dots 1$$

Where D is the ZnO crystallite size (nm), λ = 0.15418 nm, θ is the Bragg angle, and β is the full width at half maximum (FWHM). Films undergo strain ε and dislocation δ in their structure, and these parameters were calculated 12 as Eqs. 2 and 3, respectively¹⁴.

$$\varepsilon = \frac{\beta \cos \theta}{4} \dots\dots\dots 2$$

$$\delta = \frac{1}{D^2} \dots\dots\dots 3$$

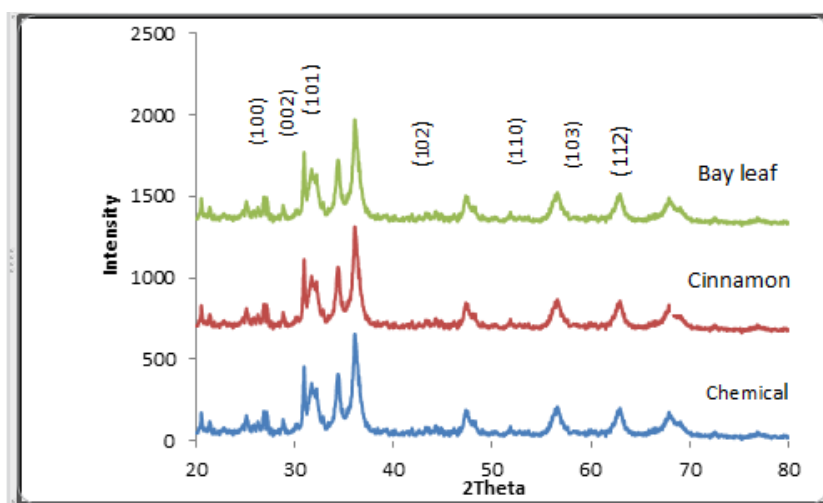


Figure 2. XRD pattern of as-synthesized ZnO using chemical method, cinnamon, and bay leaf

Table 1. Crystallite size determined from Debye Scherrer equation

Crystal plane	2θ	FWHM	B(rad)	Crystallite size D(nm)	$\epsilon \times 10^{14} \text{ lines.m}^{-2}$	$\delta \text{ strain } (\times 10^{-3})$
(100)	31.7	0.437	0.0076	25.38	12.7	0.71
(002)	34.3	0.385	0.0067	25.60	17.361	0.81
(101)	36.2	0.437	0.0076	23.13	17.36	1.49
(102)	47.3	0.613	0.0107	18.16	30.86	2.01
(110)	56	0.642	0.0112	18.06	30.36	1.98
(103)	62.4	0.689	0.0120	17.51	23.41	1.1
(112)	67.8	0.611	0.0110	19.68	25	0.9

Optical Properties

Fig 3 illustrates the recorded absorption intensity of the synthesized ZnO NPs within the wavelength range of 300 to 900 nm. The literature²¹⁻²⁴ confirms the optimum ranges of 355 to 380 nm for ZnO NPs prepared using the chemical method, cinnamon, and bay leaf. It was observed that with the high absorbance peak by use of bay leaf, the calculated band gap energy of ZnO NPs was (3.05-3.1) eV, which is comparable to the reported band gap energy of ZnO wide band gap (3.05 to 3.12 eV) as utilized in Fig 4. The creation of smaller NPs is indicated by a bigger band gap, but it also means that electron mobility is more restricted. Using bay leaf is therefore recommended since it has a higher absorbance, which could account for some of its improved photocatalytic activity. These findings predominantly validate the formation of ZnO nanoparticles via our methods.

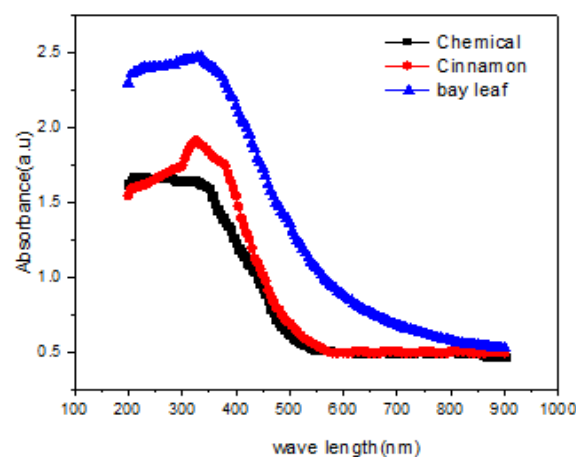


Figure 3. Absorbance of as-synthesized ZnO using chemical method, cinnamon, and bay leaf.

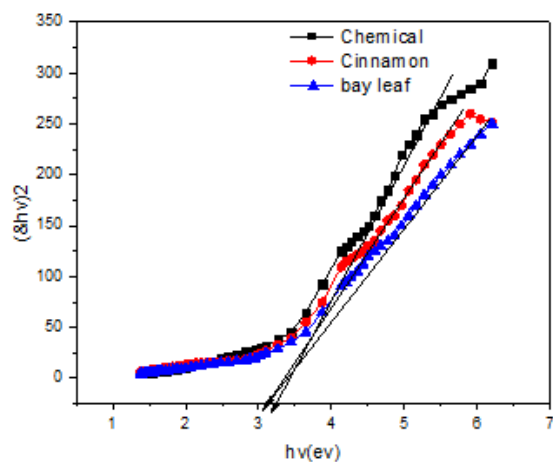


Figure 4. $(n-1)^2$ for ZnO NPs with photon energy

Compositional analysis and Surface Morphology

As shown in Fig 5(a,b and c), FESEM images were captured at various magnifications to investigate the shape and size of the synthesized nanoparticles. The main reason for the agglomeration of the nanoparticles is the extremely high surface area to volume ratio of nanoparticles. In addition to ZnO preparation methods that can affect this ratio.

A comparison of the ZnO nanoparticles' surface morphology reveals that different surface morphologies were the consequence of the technique variation. Procedure (a), wherein a solution was mixed with the zinc precursor of cinnamomum verum extract, Whereas procedure (b), in which the Zinc precursor was added to the solution of bay leaf extract, the pH of the solution was 12, yielded a

rugged surface morphology and aggregation of nanoparticles, whereas in procedure (c), in which the zinc precursor was synthesized chemically. The agglomerated form of some nanoparticles is seen to be spherical and others are irregular in shape, with an average particle diameter of 20nm, as indicated by the X-ray diffraction (XRD) results^{19, 25}.

The EDX analysis exhibited a strong signal for both Zinc and Oxygen, thereby confirming the existence of zinc oxide. The elemental composition of the analyte was determined through the use of Energy Dispersive X-ray Spectroscopy (EDX). In this process, a Zinc precursor was introduced into a solution containing cinnamon extract, resulting in prominent peaks indicating a composition of 76.9% Zinc and 23.1% Oxygen. Similarly, the Zinc precursor was added to a solution containing bay leaf extract, leading to strong peaks representing a composition of 70.7% Zinc and 29.3% Oxygen. Additionally, the Zinc precursor was introduced to a solution prepared using chemical methods, resulting in a yet to be specified composition.

A prominent peak was observed at 1eV for Zinc about Oxygen, while a discernible signal was detected at 0.5eV.

The aforementioned values are specific to the elements Zinc and Oxygen, hence supporting the elemental composition of the synthesized molecule. Fig 5 (a,band c) provides evidence of the existence of minute quantities of gold, sodium and Carbon alongside zinc and oxygen as Impurities.

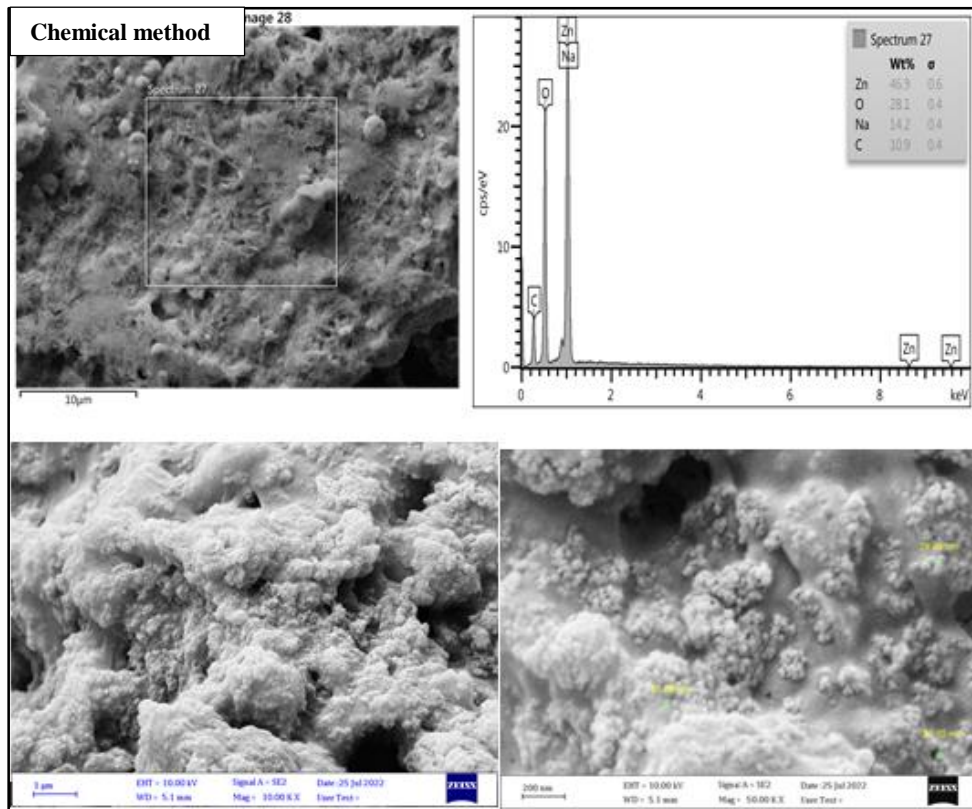


Figure 5a. Scanning electron microscopy images and EDX spectra of ZnO prepared by chemical technique.

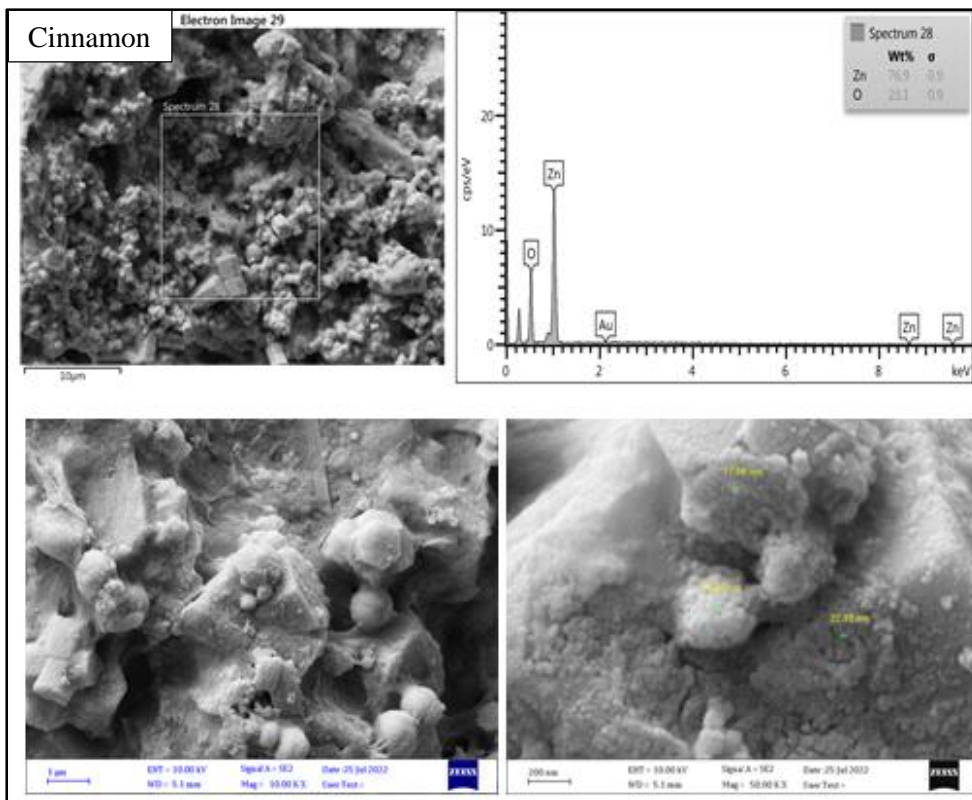


Figure 5b. Scanning electron microscopy images and EDX spectra of ZnO prepared by cinnamon extract technique.

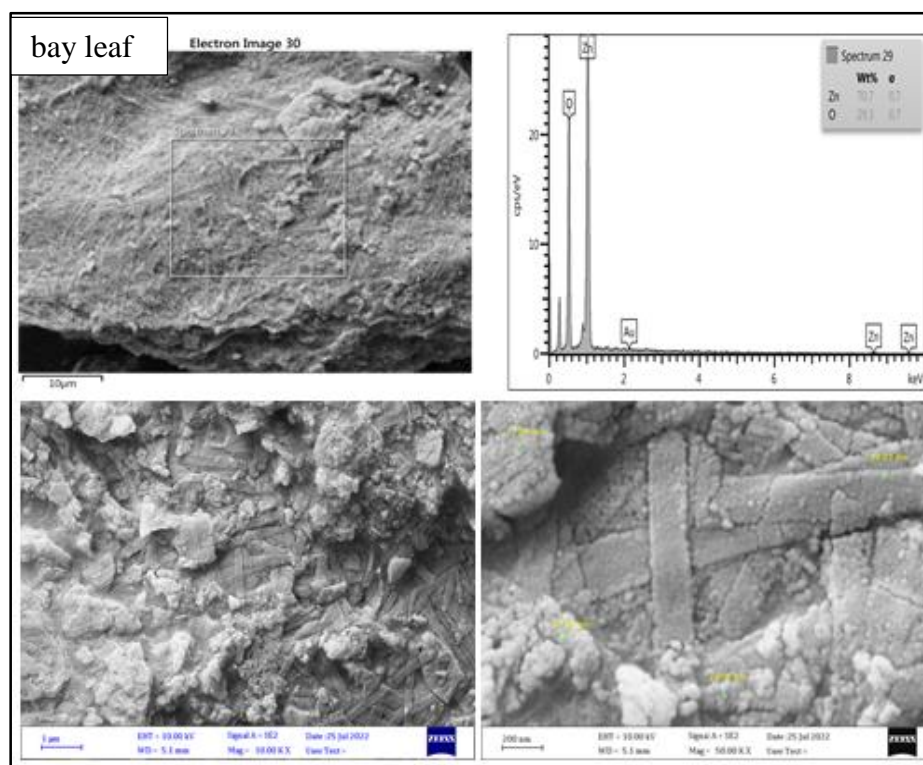


Figure 5c. Scanning electron microscopy images and EDX spectra of ZnO prepared by bay leaf extract technique.

FTIR analysis

Fourier-transform infrared spectroscopy (FT-IR) is employed to analyze the composition and development of functional groups in synthesized zinc oxide (ZnO) nanoparticles. Moreover, it posits that the synthesis of ZnO nanoparticles can be attributed to the interaction between phenolic chemicals.

Flavonoids, alkynes, and terpenoids are categorized as organic compounds. Fig 6 depicts the FT-IR spectra of synthesized ZnO nanoparticles. The functional groups converted zinc ions to ZnO, as observed by the bands. Each band represents a distinct mode of elongation.

FT-IR spectroscopy measurements are conducted to verify the existence/creation of the Zn–O bond and to ascertain the photo components enclosed on the surface of ZnO-NPs. The Fourier transform infrared spectroscopy analysis was conducted on a Bruker Alpha FTIR instrument²⁶. The FT-IR spectra of green ZnO-NPs, which were synthesized, are illustrated in Fig 9.

The peak near 2354 cm⁻¹ is attributable to a C–H stretch. C=O stretching is responsible for the peak near 1575 cm⁻¹. C = C was responsible for the peaks at 1568, 1411, and 1100 cm⁻¹.

The band seen in this study is attributed to the stretching vibrations of C–N bonds in amines, as reported by reference²⁷. The stretching vibrations of C–O in esters and carboxylic functional groups are observed throughout the spectral range of 1000 to 1300 cm⁻¹. Additionally, the occurrence of several sharp peaks at 491 cm⁻¹ and 435 cm⁻¹ is ascribed to the existence of stretching bands Zn–O.^{28,29} The intense vibrational bands at 671cm⁻¹ are attributed to the stretching modes of ZnO nanoparticle formation. By maintaining the nanoparticles' surface throughout synthesis, phytoconstituents of cinnamon extract, bay leaf extract, and compounds protect ZnO-NPs from aggregation, as determined by FT-IR.

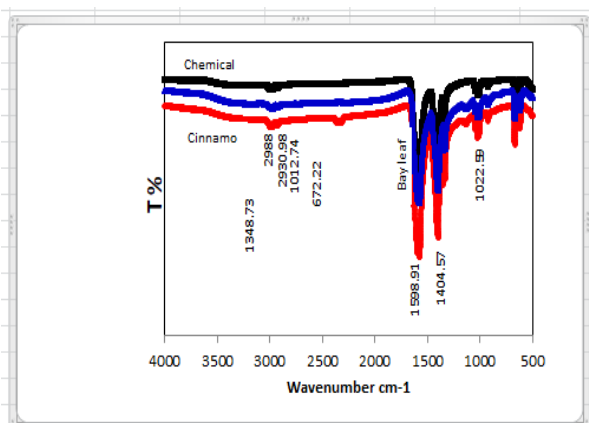


Figure 6. FTIR spectrum of ZnO nanoparticles

Photocatalytic activity of ZnO

The effectiveness of as-synthesized ZnO NPs on the degradation of methylene blue (MB), a typical model water contaminant, under solar radiation was investigated. Nanoparticle photocatalytic activity is influenced by a variety of parameters, including surface area, size, radiation sources, etc. Fig 7(a,b,c) illustrates the absorbance spectrum of ZnO thin films and the photocatalytic dye degradation activity of ZnO NPs against MB. As the irradiation time increases 15 min every-time, the maximum absorption peak of MB decreases. It is possible to observe the total degradation of MB over 1 hour. The optimal absorbance peak of MB at 275 and 660 nm was chosen to examine the depletion in absorbance at various time intervals³⁰⁻³². It can be concluded that the prepared ZnO could be used as photocatalysts in the dye degradation process.

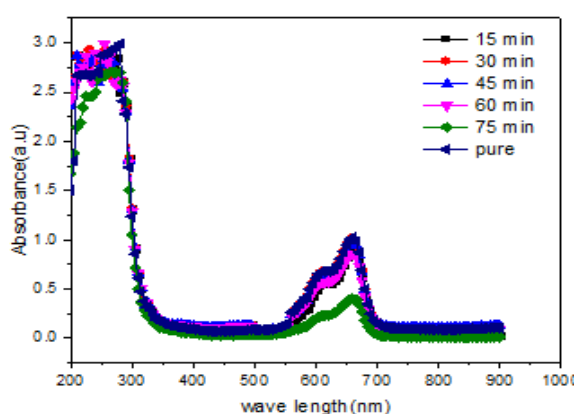


Figure 7a. UV-VIS absorption spectra demonstrate the progression of MB dye photodegradation over time using chemical method.

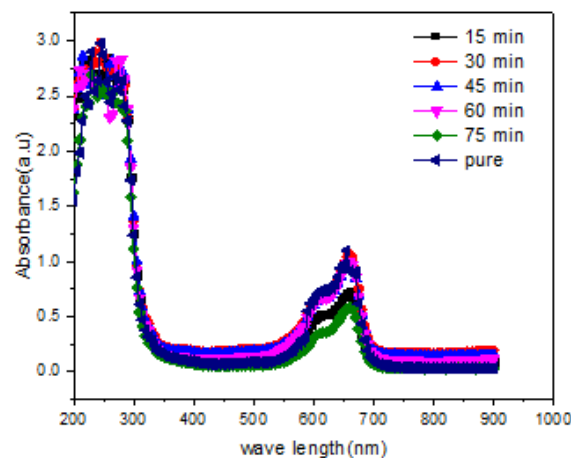


Figure 7b. UV-VIS absorption spectra demonstrate the progression of MB dye photodegradation over time using the cinnamon extract method.

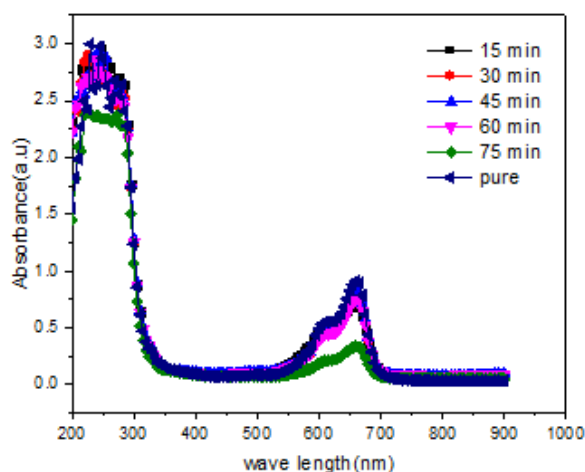


Figure 7c. UV-VIS absorption spectra demonstrate the progression of MB dye photodegradation over time using the bay leaf extract method.

Conclusion

Investigations have been done on how methods are prepared using Cinnamon extract, bay leaf extract, and chemical methods affect the structure and optical characteristics of ZnO. Using Scherrer's equation, the crystallite sizes of all samples were found to be in the nanometer range. The UV-visible spectrophotometer was used to analyze the samples' optical characteristics. Using Cinnamon extract, bay leaf extract, and by chemical method see the structure, optical characteristics, and photocatalytic activities of ZnO. Scanning electron microscopy research has shown that the typical grain sizes for various samples range from 20 nm to 60 nm; however, these sizes are not very constant, and EDX tests were used to determine the purity and composition of the samples. ZnO nanoparticles had

a 3.12 eV energy gap by chemical methods. Comparing the samples 3.08 eV using bay leaf extract and 3.05 eV using Cinnamon extract, they showed better optical characteristics. All samples demonstrated increased photocatalytic activity, suggesting enhanced MB adsorption, but the best photocatalytic activity was for the sample prepared with a leaf. There was also a slight reduction in the energy gap. Thus, this study signifies a simple cheap and eco-friendly way to synthesize ZnO-NPs from the cinnamon extract and bay leaf, and how to use them as a green photocatalyst for practical uses. Furthermore, the results showed a clear effect of green roads on optical properties, as an increase in absorbance and a decrease in the energy gap were observed.

Acknowledgment

The authors thank the College of Science Physics Department of the University of Mustansyriah for providing its laboratory facilities.

We would like to thank everyone for their participation in any manner with this initiative.

Authors' Declaration

- Conflicts of Interest: None.
- We hereby confirm that all the Figures and Tables in the manuscript are ours. Furthermore, any Figures and images, that are not ours, have been included with the necessary permission for re-publication, which is attached to the manuscript.

- No animal studies are present in the manuscript.
- No human studies are present in the manuscript.
- Ethical Clearance: The project was approved by the local ethical committee at University of Mustansyriah.

Authors' Contribution Statement

All authors contributed to the completion of this work. N. J. Gh. and N. A. H., preparing the samples and performing the tests. A. A. B. wrote the

manuscript, analysis the data and evaluated the information.

References

1. Sardar S, Munawar T, Mukhtar F, Nadeem MS, Khan SA, et al. Fullerene triggered energy storage and photocatalytic ability of La₂O₃-ZnO@C₆₀ core-shell nanocomposite: Mater Sci Eng B.2023; 288: 116151. <https://doi.org/10.1016/j.mseb.2022.116151>
2. Abbas NK, Shanan ZJ, Mohammed .H. Physical properties of Cu doped ZnO nanocrystalline thin films, Baghdad Sci J. 2022; 19(1): 217–224. <http://dx.doi.org/10.21123/bsj.2022.19.1.0217>
3. Hussain N A, Dakhil O A, Abbas L Y. Evaluation of the effect of Ag-doping ZnO microstructure on optical and structural properties and application in photocatalytic properties. MJS. 2023; 34 (3): 108-114. <http://doi.org/10.23851/mjs.v34i3.1291>
4. Abbas NK, Abdulameer AF, Ali RM, Alwash SM. The Effect of Heat Treatment on Optical properties of Copper (II) Phthalocyanine Tetrasulfonic Acid Tetrasodium Salt (CuPcTs) Organic Thin Films.

- Silicon. 2019; 11(2): 843–855. <https://doi.org/10.1007/s12633-018-9874-4>
5. Nadeem MS, Munawar T, Mukhtar F, Rabbani AW, Khan SA, et al. Synergistic photocatalytic properties of fullerene (C60) anchored V/Cu dual-doped NiO nanocomposites for water disinfection. *Mater Sci Eng B*. 2023; 273: 116705. <https://doi.org/10.1016/j.mseb.2023.116705>
 6. Moezzi A, McDonagh AM, Cortie MB. Zinc oxide particles: Synthesis, properties and applications. *J. Chem Eng J.* 2012; 185: 1-22. <https://doi.org/10.1016/j.cej.2012.01.076>
 7. Azlina HN, Hasnidawani JN, Norita H, Surip SN. Synthesis of SiO₂ nanostructures using the sol-gel method. *Acta Phys Pol A.* 2016; 129(4): 842–844 I. <https://doi.org/10.12693/APhysPolA.129.842>
 8. Raoufi D. Synthesis and microstructural properties of ZnO nanoparticles prepared by precipitation method. *Renew Energy.* 2013; 50: 932–937. <https://doi.org/10.1016/j.renene.2012.08.076>
 9. Ashkarran AA, Irajizad A, Mahdavi SM, Ahadian MM. ZnO nanoparticles prepared by the electrical arc discharge method in water. *Mater Chem Phys.* 2009; 118(1): 6–8. <https://doi.org/10.1016/j.matchemphys.2009.07.002>
 10. Ejsmont A, Goscianska J. Hydrothermal Synthesis of ZnO Superstructures with Controlled Morphology via Temperature and PH Optimization. *Materials.* 2023; 16(4): 1641. <https://doi.org/10.3390/ma16041641>
 11. Tarasenko NN, Kornev VG, Nedelko MI, Maltanova HM, Poznyak SK, Tarasenko NV. Electric field-assisted laser ablation fabrication and assembly of zinc oxide/carbon nanocomposites into hierarchical structures for supercapacitor electrodes. *Nanoscale.* 2024; 16(1): 322-334. <https://doi.org/10.1016/j.apsusc.2023.158907>
 12. Rai RS, Bajpai V, Khan MI, Elboughdiri N, Shanableh A, et al. An eco-friendly approach on green synthesis, bio-engineering applications, and future outlook of ZnO nanomaterial: A critical review. *Environ Res.* 2023; 221: 114807. <https://doi.org/10.1016/j.envres.2022.114807>
 13. Singh J, Dutta T, Kim KH, Rawat M, Samddar P, Kumar P. Green' synthesis of metals and their oxide nanoparticles: applications for environmental remediation. *J Nanobiotechnology.* 2018; 16: 84. <https://doi.org/10.1155/2010/745120>
 14. Al-Zahrani SA, Patil MB, Mathad SN, Patil AY, Otaibi AA, et al. Photocatalytic Degradation of Textile Orange 16 Reactive Dye by ZnO Nanoparticles Synthesized via Green Route Using Punica Granatum Leaf Extract. *Crystals.* 2023; 13(2): 172. <https://doi.org/10.3390/cryst13020172>
 15. Hassan SS, El Azab WI, Ali HR, Mansour MS. Green synthesis and characterization of ZnO nanoparticles for photocatalytic degradation of anthracene. *Adv Nat Sci Nanosci Nanotechnol.* 2015; 6(4): 045012. <https://doi.org/10.1088/2043-6262/6/4/045012>
 16. Bhuyan T, Mishra K, Khanuja M, Prasad R, Varma A. Biosynthesis of zinc oxide nanoparticles from *Azadirachta indica* for antibacterial and photocatalytic applications. *Mater Sci Semicond Process.* 2015; 32: 55–61. <https://doi.org/10.1016/j.mssp.2014.12.053>
 17. Davar F, Majedi A, Mirzaei A. Green synthesis of ZnO nanoparticles and their application in the degradation of some dyes. *J Am Ceram Soc.* 2015; 98(6): 1739–1746. <https://doi.org/10.1111/jace.13467>
 18. Faisal S, Jan H, Shah SA, Shah S, Khan A, et al. A Green synthesis of zinc oxide (ZnO) nanoparticles using aqueous fruit extract of *Myristica fragrans*: their characterizations and biological and environmental applications. *ACS Omega.* 2021; 6(14): 9709–9722. <https://doi.org/10.1021/acsomega.1c00310>
 19. Alharthi FA, Alghamdi AA, Alothman AA, Almarhoon ZM, Alsulaiman MF. Green synthesis of ZnO nanostructures using *Salvadora Persica* leaf extract: applications for photocatalytic degradation of methylene blue dye. *Crystals.* 2020; 10(6): 441. <http://dx.doi.org/10.3390/cryst10060441>
 20. Nadeem MS, Munawar T, Mukhtar F, Rabbani AW, Ur Rehman N, et al. Facile synthesis of PANI and rGO supported Y/Pr co-doped ZnO: boosted solar light-driven photocatalysis. *Appl Phys A.* 2023; 129(6): 450. <https://doi.org/10.1007/s00339-023-06701-2>
 21. Balouiri M, Sadiki M, Ibsouda SK. Methods for in vitro evaluating antimicrobial activity: A review. *J Pharm Anal.* 2016; 6(2): 71-79. <https://doi.org/10.1016/j.jpha.2015.11.005>
 22. Rahman MM, Islam MB, Biswas M, Khurshid Alam AH. In vitro antioxidant and free radical scavenging activity of different parts of *Tabebuia pallida* growing in Bangladesh. *BMC Res Notes.* 2015; 8(1): 1–9. <http://doi:10.1186/s13104-015-1618-6>
 23. Yung MMN, Mouneyrac C, Leung KMY. Ecotoxicity of zinc oxide nanoparticles in the marine environment. *Encyclo. Nanotech.* 2014; 1–17. http://doi:10.1007/978-94-007-6178-0_100970-1
 24. Akhil K, Khan SS. Effect of humic acid on the toxicity of bare and capped ZnO nanoparticles on bacteria, algal and crustacean systems. *J Photochem Photobiol B Biol.* 2016; 167: 136-149. <https://doi.org/10.1016/j.jphotobiol.2016.12.010>
 25. Singh K, Singh J, Rawat M. Green synthesis of zinc oxide nanoparticles using *Punica Granatum* leaf extract and its application towards photocatalytic degradation of Coomassie brilliant blue R-250 dye. *SN Appl Sci.* 2019; 1: 1-8. <https://doi.org/10.1007/s42452-019-0610-5>
 26. Jayachandran A, Aswathy TR, Nair AS. Green synthesis and characterization of zinc oxide nanoparticles using *Cayratia pedata* leaf extract. *Biochem Biophys Rep.* 2021; 26: 100995. <https://doi.org/10.1016/j.bbrep.2021.100995>

27. Ghdeeb NJ, Mohammed AH, Majeed AM. The Anti-proliferative Activity of Factory Wastes Nanoparticles against Uterus Cancer Cells: In-vitro Study. *Nano Biomed Eng.* 2022; 14(2): 149-158. <https://doi.org/10.5101/nbe.v14i2.p149-158>
28. Sirdeshpande KD, Sridhar A, Cholkar KM, Selvaraj R. Structural characterization of mesoporous magnetite nanoparticles synthesized using the leaf extract of *Calliandra haematocephala* and their photocatalytic degradation of malachite green dye. *Appl. Nanosci.* 2018; 8: 675-683. <https://doi.org/10.1016/j.arabjc.2014.09.006>
29. Chen C, Yu B, Liu P, Liu J, Wang L. Investigation of nano-sized ZnO particles fabricated by various synthesis routes. *J Ceram Process Res.* 2011; 12(4): 420-425. <http://dx.doi.org/10.36410/jcpr.2011.12.4.420>
30. Lu J, Batjikh I, Hurh J, Han Y, Ali H, et al. Photocatalytic degradation of methylene blue using biosynthesized zinc oxide nanoparticles from bark extract of *Kalopanax septemlobus*. *Optik.* 2019; 182: 980-985. <https://doi.org/10.1016/j.ijleo.2018.12.016>
31. Nusseif AD, Hussain NA, Sabry RS. Preparation and Wettability of Zinc Oxide Nanostructures by Oxidation of Zinc Foil in Hot Water. *Iraqi J Appl Phys.* 2023; 19 (4A): 67-72. <https://www.iasj.net/iasj/download/4824e968123f3363>
32. Carmona-Carmona AJ, Mora ES, Flores JI, Márquez-Beltrán C, Castañeda-Antonio MD, et al. Photocatalytic Degradation of Methylene Blue by Magnetic Opal/Fe₃O₄ Colloidal Crystals under Visible Light Irradiation. *Photochem.* 2023; 3: 390-407. <https://doi.org/10.3390/photochem3040024>

التحلل الضوئي لصبغة الميثيلين الزرقاء باستخدام جسيمات أكسيد الزنك النانوية المحضرة بالطريقة الخضراء

انوار علي باقر¹ ، نادية جاسم غضيب² ، نضال علي حسين²

¹ قسم الفيزياء، كلية العلوم للبنات، جامعة بغداد، بغداد، العراق.
² قسم الفيزياء، كلية العلوم، جامعة المستنصرية، بغداد، العراق.

الخلاصة

تتمتع طريقة التوليف الأخضر لإنتاج الجسيمات النانوية بالعديد من المزايا مقارنة بالطرق الفيزيائية والكيميائية بسبب تجنبها للمواد الخطرة وفعاليتها من حيث التكلفة. تصف هذه الدراسة التوليف الصديق للبيئة لجسيمات أكسيد الزنك النانوية (ZnO-NPs) باستخدام مستخلص القرفة، ومستخلص ورق الغار، والتقنيات الكيميائية. تم تحليل الخصائص المورفولوجية والهيكلية والبصرية لجسيمات أكسيد الزنك الخضراء النانوية من خلال استخدام المجهر الإلكتروني الماسح (FESEM)، ومطياف الأشعة السينية المشتتة للطاقة (EDX)، وتقنيات حيود الأشعة السينية (XRD). يكشف نمط حيود الأشعة السينية (XRD) أن جسيمات أكسيد الزنك النانوية (ZnO-NPs) تمتلك بنية بلورية، بمتوسط قطر يبلغ 20 نانومتر. تشير نتائج فحص المجهر الإلكتروني الماسح (FESEM) إلى أن جسيمات أكسيد الزنك النانوية (NPs) لها شكل كروي، بأحجام تتراوح بين 10 و30 نانومتر. تُظهر الجسيمات النانوية لأكسيد الزنك المُصنَّعة فعالية تحفيز ضوئي جديرة بالملاحظة في تحلل صبغة الميثيلين الزرقاء تحت التعرض المباشر لأشعة الشمس. لذلك، يشير هذا البحث إلى تقدم كبير في تقديم المحفز الضوئي المستدام لغرض التخلص من الأصباغ الضارة في الماء.

الكلمات المفتاحية: التخليق الكيميائي، التخليق الأخضر، الجسيمات النانوية، التحلل الضوئي أكسيد الزنك.